

Lorentz violating Hořava-Lifshitz gravity in light of new data

Nils A. Nilsson,^{a,1} Ewa Czuchry^a

^aNational Centre for Nuclear Research,
Hoża 69, 00-681 Warsaw, Poland

E-mail: albin.nilsson@ncbj.gov.pl, ewa.czuchry@ncbj.gov.pl

Abstract. We present new observational constraints on Lorentz violating Hořava-Lifshitz cosmological scenarios using an updated cosmological data set from Cosmic Microwave Background (Planck CMB), expansion rates of elliptical and lenticular galaxies, JLA compilation (Joint Light-Curve Analysis) data for Type Ia supernovae (SneIa), Baryon Acoustic Oscillations (BAO) and priors on the Hubble parameter. and a different parametrisation of the equations. Unlike in other approaches we consider the curvature parameter Ω_k as a free parameter in the analysis we considered the parameters Ω_k and ΔN_ν as completely free, which helped to place new, updated bounds on several of the theory parameters. Remarkably, the detailed balance scenario exhibits negative spatial curvature to more than 3σ , whereas for further theory generalizations we found evidence for positive spatial curvature at 1σ . This could create circumstantial evidence from observations and could be used to single out distinct formulations and scenarios.

¹Corresponding author.

Contents

1	Introduction	1
2	Hořava-Lifshitz Cosmology	2
2.1	Basics	2
2.2	Detailed Balance	4
2.2.1	Setup for Observational Constraints	5
2.3	Beyond Detailed Balance	5
2.3.1	Setup for Observational Constraints	6
3	Results and Discussion	6
3.1	Detailed Balance	6
3.2	Beyond Detailed Balance	7
4	Conclusions	8

1 Introduction

One of many challenging problems in modern theoretical physics is how to merge quantum field theory with general relativity. Attempts at formulating a quantum theory for gravitation have been made for many decades, but there is still no theory which clearly stands out from its competitors. One of the main obstacles one encounters when trying to quantise general relativity using standard techniques is that it is not a perturbatively renormalisable theory. This is indeed a serious problem as general relativity breaks down at small scales, and alternative formulations for a quantum theory of gravity have been developed in order to deal with this issue. For example, string theory and loop quantum gravity have been developed for this reason, and although these theories resolve some problems (such as singularities) they are few phenomenological channels through which to test these theories [1, 2]. Although no theory of quantum gravity is known it is possible to predict some of its features. For example, it is likely to contain the three constants c (speed of light, relativity), G (gravitational constant, gravitation), and \hbar (Planck’s constant, quantum mechanics). Using these constants, we can construct a characteristic energy scale for quantum gravity as $E_{Pl} = \sqrt{\hbar c^5/G}$. This is to be interpreted at the “frontier“ beyond which we can expect quantum gravity effects to manifest themselves. If this is indeed the case, we can only expect to find quantum gravity effects in regions with very high energy, strong gravity, and high velocities. The phenomenological avenues to probe these regions are sparse, and do not in general allow themselves to be recreated in the laboratory, so we are forced to rely on astrophysical observations. One possibility is that of TeV particle astrophysics, as observed with the next generation of telescopes. There are several scenarios in which quantum gravity effects could affect the opacity of the Universe to such high-energy particles [3, 4]. These effects would multiply with the distance, and could in principle be detectable with (for example) the CTA [5].

An area of observation which has recently opened up a new window to the Universe is that of *gravitational wave astronomy*. Recently, LIGO found evidence of a binary black hole merger [6], which was consistent with the prediction from general relativity for such events. Moreover, LIGO and VIRGO have also observed a binary neutron star merger [7]

which was accompanied by a short γ -ray burst picked up by the FERMI and INTEGRAL γ -ray telescopes [8]. This put strong constraints on the speed of gravitational waves, as the difference Δt from the speed of light c was found to be $-3 \cdot 10^{-15} < \Delta t/c < 7 \cdot 10^{-16}$ [9]. This new field of multimessenger astronomy has the potential to teach us more about strong gravity events and will be some of the most important ways of probing new physics in the future.

The fact that general relativity has been tested and found consistent with virtually all observations tells us that it is a very good model for the IR behaviour of quantum gravity. Thus, any candidate quantum gravity model proposed must have general relativity as its low energy limit. It therefore makes sense to look at proposals for UV-completions of general relativity, for example [10, 11]. In general these include a cutoff energy scale beyond which general relativity breaks down. If this energy scale is low enough (in the TeV range) there may be a lot of accessible phenomenology in these models. Another interesting proposal in this category is Hořava gravity, which is a concrete proposal of a UV complete theory of gravity, and possibly of quantum gravity [12, 13]. It is also referred to as Hořava-Lifshitz gravity since it contains a fixed point in the UV with an anisotropic Lifshitz scaling between space and time, explicitly breaking Lorentz invariance in the UV. A lot of work has gone into this model, including studies on cosmological solutions [14–16], dark radiation and braneworlds [16, 17], and the resolution of the initial singularity [18].

The breaking of Lorentz invariance mentioned above may seem counterintuitive, as it is one of the fundamental principles of modern physics and is strongly supported by experiment. In fact, every single experiment so far has been consistent with Lorentz invariance [19, 20]. This means that breaking Lorentz symmetry has to be done with great care. However, there is *no a priori reason* to expect that a theory of quantum gravity should uphold Lorentz invariance, as according to our understanding, spacetime takes on a quantum nature in the Planck regime, and as we have mentioned before, continuous classical spacetime emerges as a low energy limit of this quantum theory. Then, as Lorentz symmetry is a *continuous symmetry* of nature, it bears to reason that it might not exist at all in the quantum regime, but rather emerge as an IR symmetry of nature. Once Lorentz symmetry is no longer a concern, one may include higher-order derivatives in the Lagrangian in order to cure divergencies in the UV [21].

This paper is organised as follows: In Section 2 we go through brief review of Hořava-Lifshitz gravity and describe setup for observational constraints in two cases, the original one [12, 13] with detailed balance condition imposed and the one with this condition relaxed and with the generalised form of the gravitational action, the so called Sotiriou-Visser-Weinfurtner generalisation [22]. In Section 3 we present the new bounds on the theory parameters, based on a large updated cosmological dataset, and in Section 4 we show our conclusions. The details of our numerical analysis are presented in the Appendix.

2 Hořava-Lifshitz Cosmology

2.1 Basics

As we mentioned previously, one of the main obstacles on the road to quantum gravity is the fact that general relativity is non-renormalisable. This is easy to see if we notice that the expansion of any quantity \mathcal{F} in terms of the gravitational constant can be written as [21]:

$$\mathcal{F} = \sum_{n=0}^{\infty} a_n (G_N E^2)^n, \quad (2.1)$$

where E is the energy of the system, a_n is a numerical coefficient and G_N is the gravitational coupling constant. From this we see that then $E^2 \geq G^{-1}$, this expansion diverges, and it is expected that general relativity loses perturbative renormalisability at such high energies.

It is possible to improve the ultraviolet behaviour of general relativity by introducing higher-order derivative terms into the Einstein-Hilbert Lagrangian. For example, we can write it as: $S = \int d^4x \sqrt{-g}(R + R_{\mu\nu}R^{\mu\nu})$, which changes the graviton propagator from $1/k^2$ into $1/(k^2 - G_N k^4)$. The new term proportional to k^{-4} will indeed cancel the ultraviolet divergence, but the theory is now non-unitary and equipped with a massive spin-2 ghost [21]. In fact, this ghost comes from the fact that this higher-order gravity theory has time derivatives of $\mathcal{O} > 2$. In the example above, the resulting field equations are fourth order. In order to address this problem, Hořava decided to evade the ghost by constructing a higher-order theory of gravity where only the *spatial* derivatives are of $\mathcal{O} > 2$, while keeping second-order time derivatives only [12]. This requires an explicit breaking of Lorentz invariance in the ultraviolet, but to be consistent with all current experiments, which have so far failed to detect any significant signals of Lorentz invariance violation, this symmetry has to be *restored* in the infrared limit. The way Hořava overcame this hurdle was to introduce an anisotropic scaling of space and time in the ultraviolet (also known as Lifshitz scaling). This scaling takes the form (in a 4-dimensional spacetime):

$$t \rightarrow b^{-z}t, \quad x^i \rightarrow b^{-1}x^i, \quad (i = 1, 2, 3), \quad (2.2)$$

where z is a critical exponent. To restore Lorentz invariance we need to set $z = 1$, but to have power-counting renormalisability we need to have $z \geq 4$ [21]. The most common choice is to set $z = 3$. Thus, ultraviolet Lorentz violation lies at the core of Hořava-Lifshitz gravity and cosmology. Hořava assumed that it is broken down to $t \rightarrow \xi_0(t)$, $x^i \rightarrow \xi^i(t, x^k)$, which preserves the spatial diffeomorphisms. This theory acquires a symmetry group denoted $\text{Diff}[\mathcal{M}, \mathcal{F}]$, which is known as foliation-preserving diffeomorphisms [12, 21]. This allows for arbitrary changes of the spatial coordinates on each constant time slice, and also picks out a preferred time foliation of spacetime, which breaks Lorentz invariance.

Because of the anisotropic scaling between space and time, it is convenient to introduce the ADM decomposition of the spacetime metric in a preferred foliation:

$$ds^2 = -N^2 dt^2 + g_{ij}(dx^i + N^i dt)(dx^j + N^j dt), \quad (2.3)$$

where the dynamical variables of the theory now are the lapse function N , the shift vector N_i , and the spatial metric g_{ij} . Given this, we can write down the most general action for the theory as:

$$S = \int d^3x dt N \sqrt{g} [K^{ij} K_{ij} - \lambda K^2 - \mathcal{V}(g_{ij})], \quad (2.4)$$

where g is the determinant of the spatial metric g_{ij} , λ is a running coupling (dimensionless), and \mathcal{V} is a potential term. Moreover, K_{ij} is the extrinsic curvature:

$$K_{ij} = \frac{1}{2N} (\dot{g}_{ij} - \nabla_i N_j - \nabla_j N_i), \quad (2.5)$$

where an overdot denotes a full derivative with respect to the time t . The trace of K_{ij} is denoted K . The potential \mathcal{V} depends only on the spatial metric and its spatial derivatives, and is also invariant under three-dimensional diffeomorphisms [23]. It contains *only* operators of dimension 4 and 6 which can be constructed from the spatial metric g_{ij} .

2.2 Detailed Balance

A way to simplify the action (2.4) is to impose the so-called detailed balance condition, in which we assume that it should be possible to derive \mathcal{V} from a superpotential W [12, 24]:

$$\mathcal{V} = E^{ij} \mathcal{G}_{ijkl} E^{kl}, \quad E^{ij} = \frac{1}{\sqrt{g}} \frac{\delta W}{\delta g_{ij}}, \quad (2.6)$$

and

$$\mathcal{G}^{ijkl} = \frac{1}{2} \left(g^{ik} g^{jl} + g^{il} g^{jk} \right) - \lambda g^{ij} g^{kl}. \quad (2.7)$$

From this requirement, the most general action for Hořava-Lifshitz gravity is given by [24, 25]:

$$S_{ab} = \int dt d^3x \sqrt{g} N \left[\frac{2}{\kappa^2} (K_{ij} K^{ij} - \lambda K^2) + \frac{\kappa^2}{2\omega^4} C_{ij} C^{ij} - \frac{\kappa^2 \mu}{2\omega^2} \frac{\epsilon^{ijk}}{\sqrt{g}} R_{il} \nabla_j R_k^l + \frac{\kappa^2 \mu^2}{8} R_{ij} R^{ij} + \frac{\kappa^2 \mu^2}{8(1-3\lambda)} \left(\frac{1-4\lambda}{4} R^2 + \Lambda R - 3\Lambda^2 \right) \right], \quad (2.8)$$

where

$$C^{ij} = \epsilon^{ikl} \nabla_k \left(R_l^j - \frac{1}{4} R \delta_l^j \right) \quad (2.9)$$

is the Cotton tensor, ϵ^{ikl} is the totally antisymmetric tensor, and the parameters κ, ω , and μ have mass dimension $-1, 0$, and 1 , respectively [25]. It should be noted that in the action S_{ab} the analytic continuation has been carried out on the parameters μ and ω .

In order to study cosmology in this model it is necessary to populate the Universe with matter and radiation. Since we are interested in the phenomenological bounds on such a theory we will introduce a cosmological energy-momentum tensor into the modified Einstein field equations with the simple demand that the standard general relativistic expression is recovered in the infrared limit. Therefore, following the procedure in [25], we equip out Universe with a hydrodynamic approximation where p_m and ρ_m (pressure and energy density) are parameters. We also include a standard radiation component through p_r and ρ_r (note that we already have a cosmological constant Λ in S_{ab}). Moreover, we use the *projectability condition* $N = N(t)$ [12] and the standard FLRW line element (with $g_{ij} = a^2(t) \gamma_{ij}$, $N^i = 0$):

$$\gamma_{ij} dx^i dx^j = \frac{dr^2}{1 - Kr^2} + r^2 d\Omega^2, \quad (2.10)$$

where $K = \{-1, 0, 1\}$ corresponds to closed, flat, and open Universe, respectively. Therefore, we can now write down the Friedmann equations for the projectable Hořava-Lifshitz Universe under detailed-balance condition:

$$\left(\frac{\dot{a}}{a} \right)^2 = \frac{\kappa^2}{6(3\lambda - 1)} [\rho_m + \rho_r + \rho_{DE}] - \frac{\kappa^4 \mu^2 \Lambda K}{8(3\lambda - 1)^2 a^2}, \quad (2.11)$$

$$\frac{d}{dt} \frac{\dot{a}}{a} + \frac{3}{2} \left(\frac{\dot{a}}{a} \right)^2 = -\frac{\kappa^2}{4(3\lambda - 1)} [p_m + p_r + p_{DE}] - \frac{\kappa^4 \mu^2 \Lambda K}{16(3\lambda - 1)^2 a^2}. \quad (2.12)$$

Here, we have followed the procedure and notation in [25], where the authors define matter and radiation conservation equations, along with expressions for dark energy density and pressure. Now, we require that Eq. (2.10) and (2.12) coincide with the standard Friedmann equations. Thus, we can identify the following (with $c = 1$):

$$G_N = \frac{\kappa^2}{16\pi(3\lambda - 1)}, \quad \mu^2 \Lambda = \frac{1}{32\pi^2 G_N^2}. \quad (2.13)$$

2.2.1 Setup for Observational Constraints

Here we describe the theoretical setup which made it possible to constrain the parameters of the theory. Working in units where $8\pi G_N = c = 1$ we define the canonical density parameters as:

$$\Omega_m = \frac{\rho_m}{3H_0^2}, \quad \Omega_r = \frac{\rho_r}{3H_0^2}, \quad \Omega_k = -\frac{K}{H_0^2 a^2}, \quad (2.14)$$

where H_0 is the Hubble parameter as measured today. In our Markov-Chain-Monte-Carlo method we introduced a prior on H_0 , but left it otherwise unconstrained. Using these parameter to rewrite the Friedmann equation we encounter the following term: $a^{-4}\Omega_k^2 H_0^2/2\Lambda$, which is the coefficient of dark radiation in Hořava-Lifshitz. We can conveniently express this in terms of the effective number of neutrino species present in the BBN epoque. This is because the dark radiation must have been present during that time and is thus subject to BBN constraints from other experiments. As such, following [25], we can obtain a constraint equation for the dark radiation component [26, 27]:

$$\frac{\Omega_k^2 H_0^2}{2\Lambda} = 0.135\Delta N_\nu \Omega_r, \quad (2.15)$$

where ΔN_ν is the deviation of the effective number of massless neutrino species from the standard BBN value. Through the relation (2.15) we see that $\Delta N_\nu = 0$ leads to the possibility of a flat Universe. This is concerning, since it has been established that a flat Hořava-Lifshitz coincide with the standard Λ CDM model [15, 16]. Therefore the constraints on the curvature parameter Ω_k and the BBN neutrino parameter ΔN_ν are of utmost importance, and they have been left as free parameters in our analysis. That is, we have not imposed the BBN limit on ΔN_ν , but the limits we found on this parameter automatically satisfied the BBN constraint. Now, since all the density parameter have to add up to unity we have [25]:

$$1 - \Omega_m - \Omega_r - \Omega_k + \frac{\Omega_k^2}{4 \cdot 0.135\Delta N_\nu \Omega_r} + 0.135\Delta N_\nu \Omega_r = 1, \quad (2.16)$$

and we can rewrite the Friedmann equation (2.10) as:

$$\left(\frac{\dot{a}}{a}\right)^2 = H_0^2 \left[\Omega_m a^{-3} + \Omega_r (1+z)^4 + \Omega_k a^{-2} + \frac{\Omega_k^2}{4 \cdot 0.135\Delta N_\nu \Omega_r} + 0.135\Delta N_\nu \Omega_r a^{-4} \right], \quad (2.17)$$

and this is the equation that we have used in our MCMC analysis of detailed balance.

2.3 Beyond Detailed Balance

Since there has been a discussion in the literature about whether detailed balance is too restrictive ([15, 16, 21]) it is important to investigate the case when we do not impose this condition. When we relax the detailed balance condition we open up for including more terms into the potential \mathcal{V} . In this case, the Friedmann equations can be expressed as [24, 25, 28]:

$$\left(\frac{\dot{a}}{a}\right)^2 = \frac{2\sigma_0}{3\lambda-1}(\rho_m + \rho_r) + \frac{2}{3\lambda-1} \left[\frac{\sigma_1}{6} + \frac{\sigma_3 K^2}{6a^4} + \frac{\sigma_4 K}{6a^6} \right] + \frac{\sigma_2}{3(3\lambda-1)} \frac{K}{a^2}, \quad (2.18)$$

$$\frac{d}{dt} \frac{\dot{a}}{a} + \frac{3}{2} \left(\frac{\dot{a}}{a}\right)^2 = -\frac{3\sigma_0}{3\lambda-1} \frac{\rho_r}{3} - \frac{3}{3\lambda-1} \left[-\frac{\sigma_1}{6} + \frac{\sigma_3 K^2}{18a^4} + \frac{\sigma_4 K}{6a^6} \right] + \frac{\sigma_2}{6(3\lambda-1)} \frac{K}{a^2}, \quad (2.19)$$

where σ_i are arbitrary constants ($\sigma_2 < 0$) and in analogy with the detailed balance scenario [25]:

$$G_N = \frac{6\sigma_0}{8\pi(3\lambda-1)}, \quad \sigma_2 = -3(3\lambda-1). \quad (2.20)$$

2.3.1 Setup for Observational Constraints

Here, we follow the setup for the detailed balance scenario, with $8\pi G = c = 1$, and the same definition of the density parameters (Ω_X). Following the notation in [25] we introduce the following parameters:

$$\omega_1 = \frac{\sigma_1}{6H_0^2}, \quad \omega_3 = \frac{\sigma_3 H_0^2 \Omega_k}{6}, \quad \omega_4 = -\frac{\sigma_4 \Omega_k}{6}, \quad (2.21)$$

and introducing the following Bing Bang nucleosynthesis (BBN) constraint [25, 26]:

$$\omega_3 + \omega_4(1 + z_{BBN})^2 = 0.135 \Delta N_\nu \Omega_r, \quad (2.22)$$

where z_{BBN} is the redshift at BBN ($\sim 4 \cdot 10^8$). Moreover, we have the following constraint on the density parameters:

$$\Omega_m + \Omega_r + \Omega_k + \omega_1 + \omega_3 + \omega_4 = 1. \quad (2.23)$$

Using the above two equations to eliminate ω_4 along with the σ -parameters, we can rewrite the Friedmann equation (2.18) for the beyond detailed balance scenario as:

$$\left(\frac{\dot{a}}{a}\right)^2 = \Omega_m a^{-3} + (\Omega_r + \omega_3) a^{-4} + \Omega_k a^{-2} + \omega_1 + \frac{0.135 \cdot \Delta N_\nu \Omega_r - \omega_3}{(1 + z_{BBN})^2} a^{-6}. \quad (2.24)$$

This is the equation we have used in our MCMC analysis of the beyond detailed balance scenario.

3 Results and Discussion

Using the equations (2.10) and (2.18) as a starting point, we now want to find the parameter set which best fits the data. To do this we use a large updated data set with CMB (Planck), SN1a, BAO and more (see Appendix for details). In order to do this, we used a Markov-Chain Monte Carlo (MCMC) method, which was evaluated on the CIS computer cluster. The parameters are completely unconstrained but are given initial guesses, which speed up computation if they are chosen well. During every step in the computation, the MCMC method calculates the χ^2 , and in the end returns the parameter set which minimised the χ^2 function. This way, we are able to glean information about the posterior probability distribution without knowing it explicitly. For full details about the data and method, see Appendix.

3.1 Detailed Balance

To derive the constraints on the detailed balance scenario, we used Eq. (2.17) and (2.17) in our MCMC method. As the detailed balance equations are relatively simple there was no need to introduce many constraints, and the parameters ΔN_ν has been left completely free in this section. One interesting result is that we find significant evidence for *positive spatial curvature* at 3σ confidence (see Figure 1). This is an encouraging prospective observational signal, since any measurement of positive spatial curvature would be a step towards validating this model. Parameters with 1σ limits are presented in Table 1. Note that matter density parameter Ω_m displays a best-fit value of 0.454 which is quite large. This is not necessarily a drawback since it could further substantiate (or refute) the model. Also, we express the parameter Λ as Λ/H_0^2 , avoiding having to choose units for the Hubble parameter. When chosen, it is straightforward to find the parameter μ through $\mu^2 \Lambda = 2$.

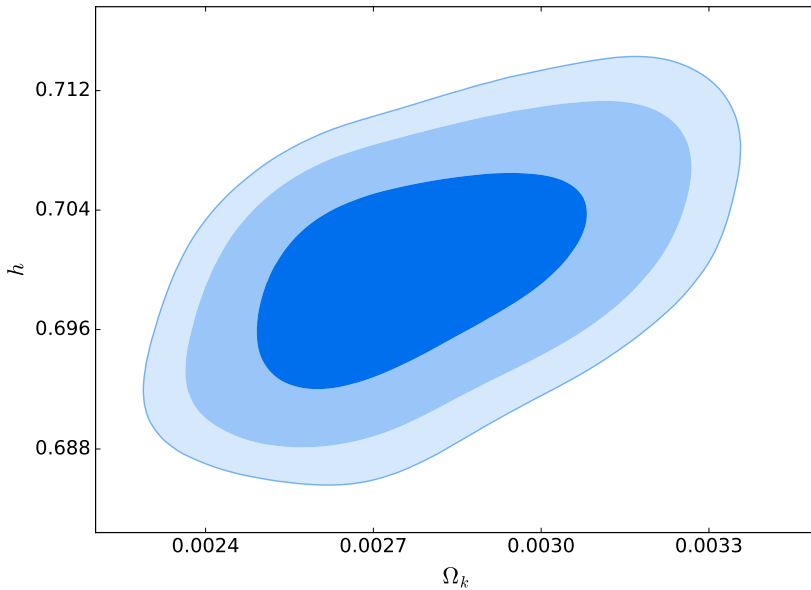


Figure 1. 1, 2, and 3σ contours of the curvature parameter Ω_k and the dimensionless Hubble parameter h under detailed balance. Spatial flatness ($\Omega_k = 0$) is excluded at more than 3σ .

Parameter	1σ limits
Ω_k	$0.00278^{+0.00017}_{-0.00022}$
h	0.6999 ± 0.0047
ΔN_ν	$0.302^{+0.034}_{-0.022}$
Ω_r	0.0000887 ± 0.0000013
Ω_m	$0.454^{+0.13}_{-0.098}$
Λ/H_0^2	$1.09^{+0.20}_{-0.26}$

Table 1. Detailed balance

3.2 Beyond Detailed Balance

To obtain constraints on parameters in the beyond detailed balance scenario we used equations (2.22), (2.23), and (2.24) in the same MCMC method as for detailed balance. Here, we introduced another constraint equation in order to make sure that the Hubble parameter is always completely real. From equation (2.22) and (2.24) it is possible to identify a generalised dark energy density [25]. As such, this energy density has to be larger than zero. In this way we obtain real values of the Hubble parameters while only making physical assumptions. The constraint can be written as:

$$\rho_{DE} = \omega_1 + \omega_3 a^{-4} \frac{0.135 \cdot \Delta N_\nu \Omega_r - \omega_3}{(1 + z_{BBN})^2} a^{-6} > 0. \quad (3.1)$$

Using the equations and constraints mentioned above we carried out an MCMC analysis of the beyond detailed balance model. All the results are shown in Table 2. Here, it is

interesting to note that in this scenario we find evidence for negative spatial curvature at 1σ : $\Omega_k = -0.0033 \pm 0.0020$. The contours showing this is plotted against h in Figure 2. This result could be used to differentiate between detailed balance and this model, since for detailed balance we found strong evidence of *positive* spatial curvature. Moreover, the parameter $\sigma_3 H_0^2$ seems to acquire a log-normal distribution, and the two-sided confidence intervals for this parameter must be considered unreliable. Because of the log-normal distribution, however, it was possible to find limits on $\log \sigma_3 H_0^2$, and a histogram of this is shown in Figure 3. We express the two σ parameters as σ_1/H_0^2 and $\sigma_3 H_0^2$ (see Eq. (2.21)) as there is no need to specify units or value for H_0 .

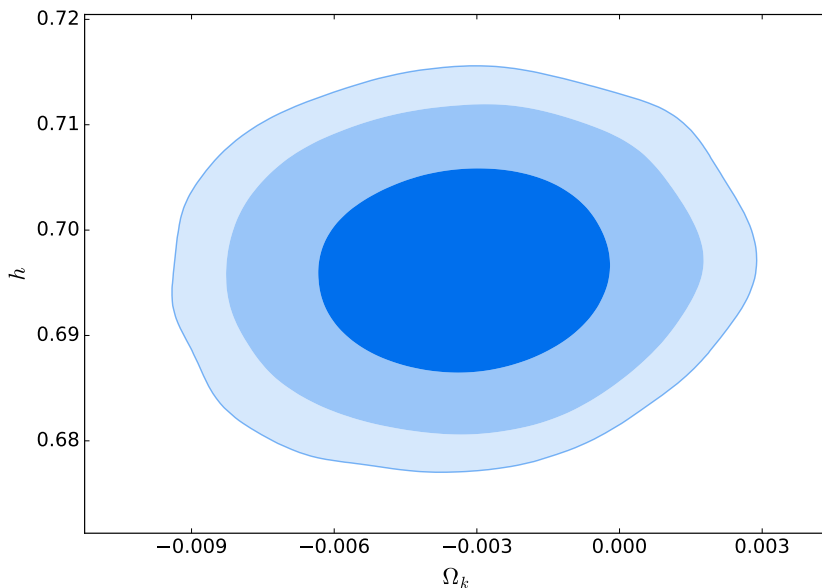


Figure 2. 1, 2, and 3σ contours of the curvature parameter Ω_k and the dimensionless Hubble parameter h . Spatial flatness is excluded at 1σ .

4 Conclusions

Using an updated cosmological data set we calculated new observational constraints on cosmological parameters of different formulations of Hořava-Lifshitz gravity. Unlike in the previous approaches [25] we use a different parametrisation of our parameters, the most important one is treating Ω_k (together with ΔN_ν) as completely free parameter. This allowed us to avoid the splitting of considerations and calculations into two separate cases of negative and positive curvature parameters that was used before.

We investigated two basic Hořava-Lifshitz scenarios, the one with detailed balance condition imposed in the action and the other one, the so called Sotiriou-Visser-Weinertner (SVW) generalization [22], which relaxes this condition and assumes higher order, i.e. cubic terms in the action. We found very remarkable results, namely detailed balance scenario exhibits negative spatial curvature to more than 3σ whereas for the SVW generalization there is

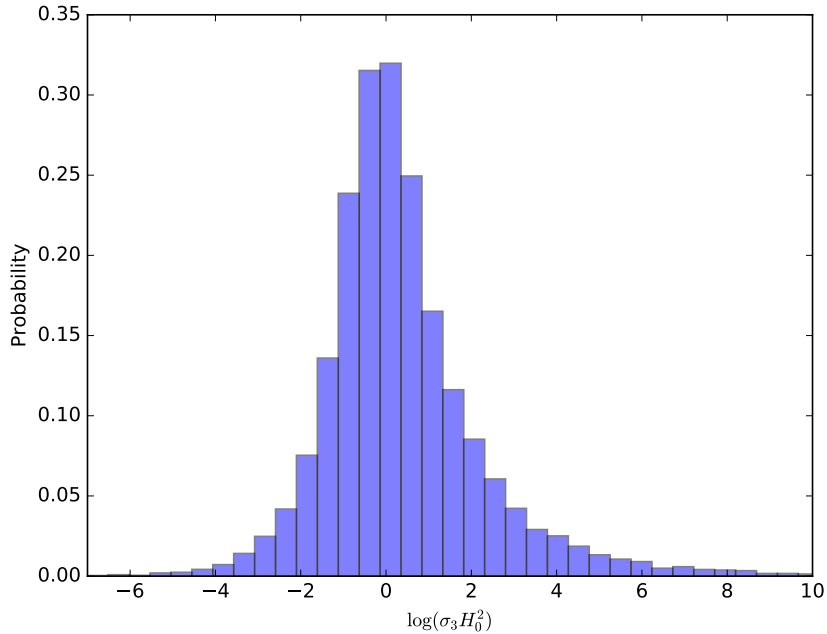


Figure 3. Normalised histogram of the parameter $\log(\sigma_3 H_0^2)$. The slightly elongated tail on the right hand side shifts the mean away from 0.

Parameter	1σ limits
Ω_k	-0.0033 ± 0.0020
h	0.6963 ± 0.0064
ΔN_ν	$0.54^{+0.15}_{-0.21}$
Ω_r	$0.0000924^{+0.0000017}_{-0.0000021}$
Ω_m	0.3244 ± 0.0068
σ_1/H_0^2	4.073 ± 0.038
$\log \sigma_3 H_0^2$	$0.4^{+1.0}_{-1.7}$

Table 2. Beyond detailed balance

evidence for positive spatial curvature at 1σ , which could be a smoking gun for observations. Some of our parameters differ quite a lot from previous works, but as we have some different assumptions (for example, in [25] the parameter ω_3 is assumed to be positive for convenience), different values are to be expected. We leave to future work the analysis whether these parameters are physical. In this paper we merely state the results of our MCMC analysis. The best fit value of the parameter ΔN_ν (kept as a completely free parameter of the theory) at 1σ is definitely positive and within BBN limits. This excludes from both scenarios the zero-curvature flat universe and corresponds to the non-zero positive cosmological constant

Λ.

Acknowledgments

The authors wish to thank Mariusz P. Dąbrowski (University of Szczecin, NCBJ) for helpful and inspiring discussions. N.A.N. wishes to thank Vincenzo Salzano (University of Szczecin) for valuable discussion and assistance with the MCMC method. N.A.N. was supported under the Polish National Science Centre Grant DEC-2012/06/A/ST2/00395. The use of the CIŚ supercomputer at the National Centre for Nuclear Research is greatly appreciated.

Appendix: The Method

In order to estimate the values of the parameters present in Hořava-Lifshitz we used a large updated cosmological data set. The data used includes; expansion rates of elliptical and lenticular galaxies, Type Ia Supernovae, Baryon Acoustic Oscillations, Cosmic Microwave Background and priors on the Hubble parameter. All expressions below are written in the flat case ($\Omega_k = 0$) for simplicity. However, Ω_k is left as a free parameter in the MCMC analysis, and thus all equations extend to the more general case of [29].

With this in mind, the expression for the comoving distance is:

$$D_M(z) = \begin{cases} \frac{D_H}{\sqrt{\Omega_k}} \sinh\left(\sqrt{\Omega_k} \frac{D_C(z)}{D_H}\right) & \text{for } \Omega_k > 0 \\ D_C(z) & \text{for } \Omega_k = 0 \\ \frac{D_H}{\sqrt{|\Omega_k|}} \sin\left(\sqrt{|\Omega_k|} \frac{D_C(z)}{D_H}\right) & \text{for } \Omega_k < 0, \end{cases} \quad (4.1)$$

where $D_H = c_0/H_0$ is the Hubble distance, $D_C(z) = D_H \int_0^z dz'/\mathcal{E}(z')$ is the line-of-sight comoving distance, and $\mathcal{E}(z) = H(z)/H_0$. Also, luminosity distance ($D_L(z)$) and angular diameter distance ($D_A(z)$) are given by:

$$D_L(z) = (1+z)D_M(z), \quad (4.2)$$

$$D_A(z) = \frac{D_M(z)}{1+z}. \quad (4.3)$$

Hubble data

For Hubble parameter data, we use the compilation from [30], which is derived from the evolution of elliptical and lenticular galaxies at redshifts $0 < z < 1.97$. The expression for χ_H^2 is:

$$\chi_H^2 = \sum_{i=1}^{24} \frac{(H(z_i, \boldsymbol{\theta}) - H_{obs}(z_i))^2}{\sigma_H^2(z_i)}, \quad (4.4)$$

where $\boldsymbol{\theta}$ is a vector containing the parameters of the model, $H_{obs}(z_i)$ are the measured values of the Hubble constant and $\sigma_H(z_i)$ are the corresponding observational errors. We will also add a prior on the Hubble constant from [31], $H_0 = 69.6 \pm 0.7 \text{ km s}^{-1} \text{ Mpc}^{-1}$.

Type Ia Supernovae

We made use of the updated JLA compilation (Joint Light-Curve Analysis) data for Type Ia supernovae (SneIa) [32] at redshifts $0 < z < 1.39$. In this case, the χ_{SN}^2 is:

$$\chi_{SN}^2 = \Delta\boldsymbol{\mu} \cdot \mathbf{C}_{SN}^{-1} \cdot \Delta\boldsymbol{\mu}, \quad (4.5)$$

where $\Delta\boldsymbol{\mu} = \mu_{theo} - \mu_{obs}$ is the difference between theoretical and observational values of the distance modulus μ . \mathbf{C}_{SN} is the total covariance matrix. The distance modulus is written as:

$$\mu(z, \boldsymbol{\theta}) = 5 \log_{10}[D_L(z, \boldsymbol{\theta})] - \alpha X_1 + \beta \mathcal{C} + \mathcal{M}_B. \quad (4.6)$$

Here, X_1 parametrises the shape of the supernova light-curve, \mathcal{C} is the colour, and \mathcal{M}_B is a nuisance parameter [32], which together with the weighting parameters α and β are included in $\boldsymbol{\theta}$. D_L is the luminosity distance which we write as:

$$D_L(z, \boldsymbol{\theta}) = \frac{1+z}{H_0} \int_0^z \frac{dz'}{\mathcal{E}(z', \boldsymbol{\theta})}. \quad (4.7)$$

Here, and only in the Supernova analysis, do we specify $H_0 = 70 \text{ km/s Mpc}^{-1}$ [32].

Baryon Acoustic Oscillations

The total χ^2 for Baryon Acoustic Oscillations is given by:

$$\chi_{BAO}^2 = \Delta \mathcal{F}^{BAO} \cdot \mathbf{C}_{BAO}^{-1} \cdot \Delta \mathcal{F}^{BAO}, \quad (4.8)$$

where \mathcal{F}^{BAO} is different from survey to survey. In this work, we used the WiggleZ Dark Energy Survey with redshifts $z = \{0.44, 0.6, 0.73\}$ [33]. For this analysis the acoustic parameter and the Alcock-Paczynski distortion parameter are of interest. The acoustic parameter is defined as follows:

$$A(z, \boldsymbol{\theta}) = 100 \sqrt{\Omega_m} h^2 \frac{D_V(z, \boldsymbol{\theta})}{z}, \quad (4.9)$$

and the Alcock-Paczynski parameter is:

$$F(z, \boldsymbol{\theta}) = (1+z) D_A(z, \boldsymbol{\theta}) H(z, \boldsymbol{\theta}), \quad (4.10)$$

where D_A is the angular diameter distance, which is Eq. (4.3) in the case of $\Omega_k = 0$:

$$D_A(z, \boldsymbol{\theta}) = \frac{1}{H_0} \frac{1}{1+z} \int_0^z \frac{dz'}{\mathcal{E}(z', \boldsymbol{\theta})}, \quad (4.11)$$

and D_V is the geometric mean of the physical angular diameter distance D_A and the Hubble function $H(z)$. It reads as:

$$D_V(z, \boldsymbol{\theta}) = \left[(1+z)^2 D_A^2(z, \boldsymbol{\theta}) \frac{z}{H(z, \boldsymbol{\theta})} \right]^{1/3}. \quad (4.12)$$

Included in the Baryon Acoustic Oscillation analysis is also data from Sloan Digital Sky Survey (SDSS-III) Baryon Oscillation Spectroscopic Survey (BOSS) DR12 [34]. It can be written as:

$$D_M(z) \frac{r_s^{mod}(z_d)}{r_s(z_d)} \quad \text{and} \quad H(z) \frac{r_s(z_d)}{r_s^{mod}(z_d)} \quad (4.13)$$

Here, $r_s(z_d)$ represents the sound horizon at the *dragging redshift* z_d . $r_s^{mod}(z_d)$ is the same horizon, but evaluated for the given cosmological model. Here, it is used that $r_s^{mod}(z_d) = 147.78 \text{ Mpc}$ as in [34]. A good approximation of the sound horizon can be found in [35]:

$$z_d = \frac{1291(\Omega_m h^2)^{0.251}}{1 + 0.659(\Omega_m h^2)^{0.828}} \left[1 + b_1(\Omega_b h^2)^{b_2} \right], \quad (4.14)$$

where

$$\begin{aligned} b_1 &= 0.313(\Omega_m h^2)^{-0.419} [1 + 0.607(\Omega_m h^2)^{0.6748}] , \\ b_2 &= 0.238(\Omega_m h^2)^{0.223} . \end{aligned} \quad (4.15)$$

The sound horizon r_s can then be defined as:

$$r_s(z, \boldsymbol{\theta}) = \int_z^\infty \frac{c_s(z')}{H(z', \boldsymbol{\theta})} dz' , \quad (4.16)$$

and the sound speed is given by:

$$c_s(z) = \frac{1}{\sqrt{3(1 + \bar{R}_b(1+z)^{-1})}} , \quad (4.17)$$

and

$$\bar{R}_b = 31500\Omega_b h^2 (T_{CMB}/2.7)^{-4} , \quad (4.18)$$

with $T_{CMB} = 2.726$ K.

Ending the Baryon Acoustic Oscillation analysis, considered data from the Quasar-Lyman α Forest from Sloan Digital Sky Survey - Baryon Oscillation Spectroscopic Survey DR11 [36]:

$$\frac{D_A(z = 2.36)}{r_s(z_d)} = 10.8 \pm 0.4 , \quad (4.19)$$

$$\frac{1}{H(z = 2.36)r_s(z_d)} = 9.0 \pm 0.3 . \quad (4.20)$$

With the contributions mentioned throughout this section, the total χ^2 for Baryon Acoustic Oscillations will be $\chi_{BAO}^2 = \chi_{WiggleZ}^2 + \chi_{BOSS}^2 + \chi_{Lyman}^2$.

Cosmic Microwave Background

In this analysis, we write the χ^2 for the Cosmic Microwave Background (CMB) in the following way:

$$\chi_{CMB}^2 = \Delta \mathcal{F}^{CMB} \cdot \mathbf{C}_{CMB}^{-1} \cdot \Delta \mathcal{F}^{CMB} . \quad (4.21)$$

Here, \mathcal{F}^{CMB} is a vector quantity given in [37], which summarises the information available in the full power spectrum of the Cosmic Microwave Background from the 2015 Planck data release [38]. \mathcal{F}^{CMB} contains the Cosmic Microwave Background shift parameters and the baryonic density parameter. The shift parameters are:

$$\begin{aligned} R(\boldsymbol{\theta}) &\equiv \sqrt{\Omega_m H_0^2} r(z_*, \boldsymbol{\theta}) \\ l_a(\boldsymbol{\theta}) &\equiv \pi \frac{r(z_*, \boldsymbol{\theta})}{r_s(z_*, \boldsymbol{\theta})} , \end{aligned} \quad (4.22)$$

whereas the baryonic density parameter is simply $\Omega_b h^2$. As mentioned before, r_s is the comoving sound horizon at the photon-decoupling redshift z_* , which is given by [39]:

$$z_* = 1048 [1 + 0.00124(\Omega_b h^2)^{-0.738}] (1 + g_1(\Omega_m h^2)^{g_2}) , \quad (4.23)$$

with:

$$g_1 = \frac{0.0783(\Omega_b h^2)^{-0.238}}{1 + 39.5(\Omega_b h^2)^{-0.763}} , \quad (4.24)$$

$$g_2 = \frac{0.560}{1 + 21.1(\Omega_b h^2)^{1.81}} ; \quad (4.25)$$

and r is the comoving distance:

$$r(z, \boldsymbol{\theta}_b) = \frac{1}{H_0} \int_0^z \frac{dz'}{\mathcal{E}(z', \boldsymbol{\theta})} dz' . \quad (4.26)$$

All the methods mentioned above all contribute to the total χ^2 , and the function to minimise is: $\chi_{tot}^2 = \chi_{H_0}^2 + \chi_H^2 + \chi_{SN}^2 + \chi_{WiggleZ}^2 + \chi_{BOSS}^2 + \chi_{Lyman}^2 + \chi_{CMB}^2$.

References

- [1] Fernando Quevedo. Is String Phenomenology an Oxymoron? 2016.
- [2] Florian Girelli, Franz Hinterleitner, and Seth Major. Loop Quantum Gravity Phenomenology: Linking Loops to Observational Physics. *SIGMA*, 8:098, 2012. doi: 10.3842/SIGMA.2012.098.
- [3] Tadashi Kifune. Invariance violation extends the cosmic ray horizon? *Astrophys. J.*, 518: L21–L24, 1999. doi: 10.1086/312057.
- [4] R. J. Protheroe and H. Meyer. An Infrared background TeV gamma-ray crisis? *Phys. Lett.*, B493:1–6, 2000. doi: 10.1016/S0370-2693(00)01113-8.
- [5] Malcolm Fairbairn, Albin Nilsson, John Ellis, Jim Hinton, and Richard White. The CTA Sensitivity to Lorentz-Violating Effects on the Gamma-Ray Horizon. *JCAP*, 1406:005, 2014. doi: 10.1088/1475-7516/2014/06/005.
- [6] B.P. Abbott et al. Observation of Gravitational Waves from a Binary Black Hole Merger. *Phys. Rev. Lett.*, 116(6):061102, 2016. doi: 10.1103/PhysRevLett.116.061102.
- [7] B.P. Abbott et al. GW170817: Observation of Gravitational Waves from a Binary Neutron Star Inspiral. *Phys. Rev. Lett.*, 119(16):161101, 2017. doi: 10.1103/PhysRevLett.119.161101.
- [8] E. Troja et al. The X-ray counterpart to the gravitational wave event GW 170817. *Nature*, 551:71–74, 2017. doi: 10.1038/nature24290. [Nature551,71(2017)].
- [9] B. P. Abbott et al. Gravitational Waves and Gamma-rays from a Binary Neutron Star Merger: GW170817 and GRB 170817A. *Astrophys. J.*, 848(2):L13, 2017. doi: 10.3847/2041-8213/aa920c.
- [10] Nima Arkani-Hamed, Savvas Dimopoulos, and G. R. Dvali. The Hierarchy problem and new dimensions at a millimeter. *Phys. Lett.*, B429:263–272, 1998. doi: 10.1016/S0370-2693(98)00466-3.
- [11] Gia Dvali. Black Holes and Large N Species Solution to the Hierarchy Problem. *Fortsch. Phys.*, 58:528–536, 2010. doi: 10.1002/prop.201000009.
- [12] Petr Horava. Quantum Gravity at a Lifshitz Point. *Phys. Rev.*, D79:084008, 2009. doi: 10.1103/PhysRevD.79.084008.
- [13] Petr Horava and Charles M. Melby-Thompson. General Covariance in Quantum Gravity at a Lifshitz Point. *Phys. Rev.*, D82:064027, 2010. doi: 10.1103/PhysRevD.82.064027.
- [14] Shinji Mukohyama. Horava-Lifshitz Cosmology: A Review. *Class. Quant. Grav.*, 27:223101, 2010. doi: 10.1088/0264-9381/27/22/223101.

- [15] Elias Kiritsis and Georgios Kofinas. Horava-Lifshitz Cosmology. *Nucl. Phys.*, B821:467–480, 2009. doi: 10.1016/j.nuclphysb.2009.05.005.
- [16] Gianluca Calcagni. Cosmology of the Lifshitz universe. *JHEP*, 09:112, 2009. doi: 10.1088/1126-6708/2009/09/112.
- [17] Emmanuel N. Saridakis. Horava-Lifshitz Dark Energy. *Eur. Phys. J.*, C67:229–235, 2010. doi: 10.1140/epjc/s10052-010-1294-6.
- [18] Robert Brandenberger. Matter Bounce in Horava-Lifshitz Cosmology. *Phys. Rev.*, D80:043516, 2009. doi: 10.1103/PhysRevD.80.043516.
- [19] Sidney R. Coleman and Sheldon L. Glashow. High-energy tests of Lorentz invariance. *Phys. Rev.*, D59:116008, 1999. doi: 10.1103/PhysRevD.59.116008.
- [20] V. Alan Kostelecky and Neil Russell. Data Tables for Lorentz and CPT Violation. *Rev. Mod. Phys.*, 83:11–31, 2011. doi: 10.1103/RevModPhys.83.11.
- [21] Anzhong Wang. Hořava gravity at a Lifshitz point: A progress report. *Int. J. Mod. Phys.*, D26(07):1730014, 2017. doi: 10.1142/S0218271817300142.
- [22] Thomas P. Sotiriou, Matt Visser, and Silke Weinfurtner. Quantum gravity without Lorentz invariance. *JHEP*, 10:033, 2009. doi: 10.1088/1126-6708/2009/10/033.
- [23] D. Blas, O. Pujolas, and S. Sibiryakov. Consistent Extension of Horava Gravity. *Phys. Rev. Lett.*, 104:181302, 2010. doi: 10.1103/PhysRevLett.104.181302.
- [24] Thomas P. Sotiriou. Horava-Lifshitz gravity: a status report. *J. Phys. Conf. Ser.*, 283:012034, 2011. doi: 10.1088/1742-6596/283/1/012034.
- [25] Sourish Dutta and Emmanuel N. Saridakis. Observational constraints on Horava-Lifshitz cosmology. *JCAP*, 1001:013, 2010. doi: 10.1088/1475-7516/2010/01/013.
- [26] Keith A. Olive, Gary Steigman, and Terry P. Walker. Primordial nucleosynthesis: Theory and observations. *Phys. Rept.*, 333:389–407, 2000. doi: 10.1016/S0370-1573(00)00031-4.
- [27] Kaoru Hagiwara et al. Review of particle physics. Particle Data Group. *Phys. Rev.*, D66:010001, 2002. doi: 10.1103/PhysRevD.66.010001.
- [28] Christos Charmousis, Gustavo Niz, Antonio Padilla, and Paul M. Saffin. Strong coupling in Horava gravity. *JHEP*, 08:070, 2009. doi: 10.1088/1126-6708/2009/08/070.
- [29] David W. Hogg. Distance measures in cosmology. 1999.
- [30] Michele Moresco. Raising the bar: new constraints on the Hubble parameter with cosmic chronometers at $z \sim 2$. *Mon. Not. Roy. Astron. Soc.*, 450(1):L16–L20, 2015. doi: 10.1093/mnras/slv037.
- [31] C. L. Bennett, D. Larson, J. L. Weiland, and G. Hinshaw. The 1% Concordance Hubble Constant. *Astrophys. J.*, 794:135, 2014. doi: 10.1088/0004-637X/794/2/135.
- [32] M. Betoule et al. Improved cosmological constraints from a joint analysis of the SDSS-II and SNLS supernova samples. *Astron. Astrophys.*, 568:A22, 2014. doi: 10.1051/0004-6361/201423413.
- [33] Chris Blake et al. The WiggleZ Dark Energy Survey: Joint measurements of the expansion and growth history at $z < 1$. *Mon. Not. Roy. Astron. Soc.*, 425:405–414, 2012. doi: 10.1111/j.1365-2966.2012.21473.x.
- [34] Shadab Alam et al. The clustering of galaxies in the completed SDSS-III Baryon Oscillation Spectroscopic Survey: cosmological analysis of the DR12 galaxy sample. *Submitted to: Mon. Not. Roy. Astron. Soc.*, 2016.
- [35] Daniel J. Eisenstein and Wayne Hu. Baryonic features in the matter transfer function. *Astrophys. J.*, 496:605, 1998. doi: 10.1086/305424.

- [36] Andreu Font-Ribera et al. Quasar-Lyman α Forest Cross-Correlation from BOSS DR11 : Baryon Acoustic Oscillations. *JCAP*, 1405:027, 2014. doi: 10.1088/1475-7516/2014/05/027.
- [37] Yun Wang and Mi Dai. Exploring uncertainties in dark energy constraints using current observational data with Planck 2015 distance priors. *Phys. Rev.*, D94(8):083521, 2016. doi: 10.1103/PhysRevD.94.083521.
- [38] P. A. R. Ade et al. Planck 2015 results. XIII. Cosmological parameters. *Astron. Astrophys.*, 594:A13, 2016. doi: 10.1051/0004-6361/201525830.
- [39] Wayne Hu and Naoshi Sugiyama. Small scale cosmological perturbations: An Analytic approach. *Astrophys. J.*, 471:542–570, 1996. doi: 10.1086/177989.